

From Laplacian-to-Adjacency Matrix for Continuous Spins on Graphs

Nikita Titov* and Andrea Trombettoni†

Department of Physics, University of Trieste, Strada Costiera 11, 34151 Trieste, Italy

(Dated: November 18, 2025)

The study of spins and particles on graphs has many applications across different fields, from time dynamics on networks to the solution of combinatorial problems. Here, we study the large n limit of the $O(n)$ model on general graphs, which is considerably more difficult than on regular lattices. Indeed, the loss of translational invariance gives rise to an infinite set of saddle point constraints in the thermodynamic limit. We show that the free energy at low and high temperature T is determined by the spectrum of two crucial objects from graph theory: the Laplacian matrix at low T and the Adjacency matrix at high T . Their interplay is studied in several classes of graphs. For regular lattices the two coincide. We obtain an exact solution on trees, where the Lagrange multipliers interestingly depend solely on the number of nearest neighbors. For decorated lattices, the singular part of the free energy is governed by the Laplacian spectrum, whereas this is true for the full free energy only in the zero temperature limit. Finally, we discuss a bipartite fully connected graph to highlight the importance of a finite coordination number in these results. Results for quantum spin models on a loopless graph are also presented.

I. INTRODUCTION

The assumption of homogeneity is standard practice in theoretical physics, as it enables the use of Fourier transforms and greatly simplifies the analysis of many-body systems [1–3]. This assumption, however, removes the influence of underlying spatial structures. There are indeed many contexts where it is necessary to study the properties of particles or spins breaking translational invariance giving rise to new physical phenomena [4–6]. The study of properties of particles or variables on graphs finds applications in diverse areas, spanning from urban and biological networks [7] to complex systems [8], random walks [9] and statistical mechanics [10–13]. As a further motivation, recent progress in the control of trapping potentials in ultracold atomic systems using digital micromirror devices [14, 15] and holographic methods [16, 17] has enabled the realisation of finely tunable lattice geometries and energy potentials, which can also be well controlled by optical tweezer arrays [18]. By using counterpropagating laser beams one can create one-dimensional chains of Bose-Einstein condensates [19, 20], and with holographic techniques a junction of three or four one-dimensional waveguides (forming a so-called Y graph) has been constructed [21]. The counterpart of these advances in superconducting networks is provided by the possibility of connecting Josephson junctions according to a non-translational invariant topology [22–24]. These developments allow the direct study of quantum particles and the related effective spin models on controllable non-translational invariant graphs.

Beyond their experimental relevance, the study of models defined on graphs is also connected to combinatorial optimisation problems such as Maximum Cut and the Number Partitioning Problem which are generally NP-hard

* nikita.titov@units.it

† atrombettoni@units.it

and can be mapped to the ground state energy computation of the Ising model on a complex structure [25]. As an example, the most powerful algorithms for the approximation of Maximum Cut [26] are based on the relaxation of the binary Ising constraints to vectors on a sphere corresponding to $O(n)$ models from physics.

The absence of translational symmetry and the interest in studying equilibrium and dynamical properties of particles and spins on graphs motivated the development of numerical and analytical approaches [27–29]. Belief propagation provides efficient algorithms for classical systems to determine marginals of probability distributions by sending messages from site to site [6]. It has also been found that well known approaches like the Jordan-Wigner transformation, originally formulated for regular chains, can be generalised to some graphs, leading to physically relevant consequences. Quantum spin models on a Y graph can give rise to the Kondo effect through a modified Jordan-Wigner transformation [30, 31]. However, on a general graph the Jordan-Wigner transformation does not lead to a solvable model of fermions.

A prominent analytical approach is the large n expansion [32], which allows to approximate both field theories and interacting models on a lattice by a quadratic Hamiltonian subject to a saddle point constraint. It is well known that classical $O(n)$ spin models are equivalent to the so-called spherical model in the large n limit on regular lattices [33–35]. However, the assumption of translational invariance is necessary to obtain the single constraint equation of the spherical model. On general graphs the analysis is considerably more intricate [36–38]. An important result is that the universality class of the large n model on graphs is the same as the spherical one [27] and depends only on the spectral dimension [39].

In this paper, we characterize the large n limit of continuous spins on general graphs and we show that the limiting model can be formulated directly in terms of the Laplacian and Adjacency matrices of the underlying graph. The importance of determining and characterizing the model obtained in the large n limit for general graphs is that with this one can perform analytical and numerical calculations of equilibrium and dynamical quantities in a much easier way than directly dealing with the original $O(n)$ problem. The reason is that the limiting model is Gaussian. Whether the large n approximation gives good results for finite n depends on the problem at hand, but it is very useful both in giving first qualitative results and as a basis of an $1/n$ expansion.

II. THE LAPLACIAN AND ADJACENCY MATRICES

Let us introduce the two main characters of this paper. For a connected graph \mathcal{G} , the Adjacency matrix A is given by:

$$A_{ij} = \begin{cases} 1 & \text{if sites } i \text{ and } j \text{ are connected,} \\ 0 & \text{otherwise,} \end{cases} \quad (1)$$

while the Laplacian matrix L is defined as:

$$L_{ij} = \delta_{ij}z_i - A_{ij}, \quad (2)$$

where $z_i = \sum_j A_{ij}$ is the number of nearest neighbors, i.e., the coordination number of site i . The spectral properties of both of these matrices play a central role in graph theory [40–42] and determine many physical properties of the models defined on their corresponding graphs. Notice that L and A are defined on the graph, independently from the model we put on it. The main point of difference between L and A is that the Laplacian is positive semidefinite with a single zero eigenvalue and a corresponding constant eigenvector: the ground state is homogeneous in *any* graph. At variance, the ground state of the Adjacency matrix tends to localize around sites with a larger coordination number. On translationally invariant lattices these matrices share the same spectrum up to a constant shift ($z = z_i$, for each site i), while for general graphs, such as the Y graph, the difference between their low-energy properties gives rise to distinct physical properties related to the localization of particles or modes around the more connected sites [43–46]. Needless to say, the Laplacian matrix in the continuum limit for the translational invariant case gives rise to the continuum Laplacian operator $\Delta = \nabla^2$. The question we aim to answer is whether, on a general graph in the large n limit, we find the Laplacian or the Adjacency matrix. Briefly, the answer is both.

We show that the free energy of the $O(n)$ model in the large n limit is governed by the Laplacian and Adjacency spectra in different temperature limits. The Laplacian is retrieved for temperature $T \rightarrow 0$, while the Adjacency matrix for $T \rightarrow \infty$. We study the Laplacian-to-Adjacency interplay and we present analytical solutions of the saddle-point equations for several representative graphs.

III. THE MODEL

The ferromagnetic classical $O(n)$ model on a graph \mathcal{G} , with N sites, is defined by the Hamiltonian:

$$-\beta H = K \sum_{i,j=1}^N A_{ij} \mathbf{S}_i \cdot \mathbf{S}_j, \quad (3)$$

where $K = \beta J > 0$ is a dimensionless, ferromagnetic coupling and \mathbf{S}_i are n -component vectors with norm $\mathbf{S}_i \cdot \mathbf{S}_i = n$ (with $k_B = 1$ and $\beta = 1/T$). This normalization is chosen to correctly define the large n limit for regular lattices [35].

A key observation is that the model (3) is written purely in terms of the Adjacency matrix. In the seminal paper [35], Stanley proved that on regular lattices the free energy corresponding to Eq. (3) in the limit $n \rightarrow \infty$ is equal to the free energy of the spherical model. The Hamiltonian of the so-called *mean* spherical model is given by:

$$-\beta H = \sum_{i,j=1}^N S_i (K A_{ij} - \delta_{ij} \lambda) S_j, \quad (4)$$

where S_i is a real valued scalar, and the Lagrange multiplier λ is chosen such that the average spherical constraint $\langle \sum_i S_i^2 \rangle = N$ is fulfilled. The fact that only a single Lagrange multiplier is required when taking the limit arises from the equivalence of all lattice sites in a regular lattice. It is known [27, 38], that when performing the large n limit on more general graphs, it is *a priori* necessary to include as many Lagrange multipliers as there are sites such that the correct Hamiltonian in this case reads (see Appendix A):

$$-\beta H = \sum_{i,j=1}^N S_i (K A_{ij} - \delta_{ij} \lambda_i) S_j \equiv - \sum_{i,j=1}^N S_i M_{ij} S_j, \quad (5)$$

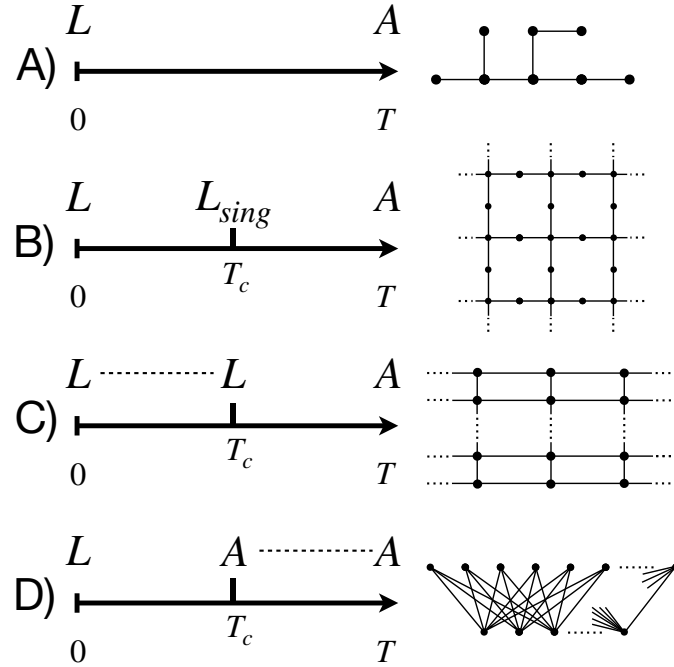


FIG. 1. Appearance of the Laplacian (denoted in the figure as "L") and Adjacency ("A") matrices for the graphs considered in the text. A) For trees there is no critical point such that one only has the high and low temperature limit. B) In the decorated lattice the singular part of the free energy is determined by the Laplacian matrix (denoting this as " L_{sing} "). C) For the strip the Laplacian matrix is retrieved in the whole low temperature regime. D) The complete bipartite graph has diverging coordination numbers and therefore does not have to obey the result in [27], instead the transition is governed by the Adjacency matrix.

and the Lagrange multipliers λ_i have to be determined by enforcing $\langle S_i^2 \rangle = 1$, for $i = 1, \dots, N$. In the thermodynamic limit one is therefore left with infinitely many constraint equations, so that explicit solutions are rare [36, 37]. It should be noted that if all λ_i are equal, the free energy connected to Eq. (5) will be determined by the eigenvalues of the Adjacency matrix shifted by a constant. If, on the other hand, $\lambda_i = K z_i$ one obtains the Laplacian matrix. Whenever all sites of the graph have the same coordination number, this difference disappears.

IV. THE HIGH- AND LOW-TEMPERATURE LIMIT

The Lagrange multipliers are determined by a set of saddle point equations for the free energy density f :

$$\frac{\partial}{\partial \lambda_i} f = 0, \quad \text{for } i = 1, \dots, N, \quad (6)$$

where as usual $\beta f = -\log Z/N$ and Z is the partition function (from now on we will refer to f as simply the free energy). In general, a closed form solution cannot be obtained since Eq. (6) requires, at minimum, knowledge of the determinant of M and its derivatives.

In the low temperature limit ($K \rightarrow \infty$), the matrix M is governed by the ground state of Eq. (5), yielding the solutions of Eq. (6) (see Appendix B):

$$\lambda_i = K z_i, \quad M_{ij} = K L_{ij}. \quad (7)$$

The eigenvalues of the Hamiltonian are therefore given by the ones of the Laplacian matrix and the Lagrange multipliers are solely determined by the number of connections per site.

For high temperatures i.e. $K \rightarrow 0$ one can calculate the partition function perturbatively which leads to:

$$\lambda_i = \frac{1}{2} + \mathcal{O}(K^2), \quad M_{ij} = \frac{1}{2}\delta_{ij} - KA_{ij}, \quad (8)$$

implying that the eigenvalues of the Adjacency matrix, shifted by a large constant such that all of them are positive, determine the free energy. The Lagrange multipliers become independent of the graph structure.

These considerations already capture the essential role of graph topology in both temperature limits. The remaining question concerns the behavior between the two limits and, if it exists, at the critical point. In [27] it was shown that the singular part of the free energy associated with Hamiltonian in Eq. (5) coincides with that of a modified spherical model on the same graph, characterized by a single Lagrange multiplier [39]:

$$\tilde{M}_{ij} = KA_{ij} + \delta_{ij}z_i\lambda, \quad (9)$$

such that the Lagrange multiplier λ enforces a generalization of the lattice constraint to graphs $\langle \sum_i z_i S_i^2 \rangle = N$. At the critical temperature $\lambda^{(c)} = K_c$. However, it is not true that the Lagrange multipliers λ_i of the model obtained in the large n limit of the $O(n)$ model satisfy $\lambda_i^{(c)} = z_i\lambda_c$ at the critical point. The following sections will illustrate the behavior of the Lagrange multipliers for different representative graphs. Our findings are summarized in Fig. 1, starting from trees that are the subject of the next section.

V. TREES

Trees are graphs without loops which makes their saddle point equations analytically tractable. We first write down the partition function:

$$Z = \int \prod_{i=1}^N dS_i \exp \left(\sum_{i,j=1}^N S_i (KA_{ij} - \delta_{ij}\lambda_i) S_j \right), \quad (10)$$

with the constraints $\langle S_i^2 \rangle = 1$. In a tree, there exists always at least one site S_k with coordination number $z_k = 1$. By integrating this site out and shifting the Lagrange multiplier of the neighboring site $\lambda_{k'}$ one can isolate all terms depending on λ_k in the partition function and solve for the corresponding Lagrange multiplier (see Appendix C for a more detailed derivation). The only effect on the other sites is a renormalization of the neighboring Lagrange multiplier. The remaining graph is still a tree and one can therefore repeat this procedure iteratively for all sites. In the end, the Lagrange multipliers for any tree depend solely on the number of nearest neighbors and take the final form:

$$\lambda_i = \frac{1}{2} + \frac{z_i}{4} \left(-1 + \sqrt{1 + 16K^2} \right). \quad (11)$$

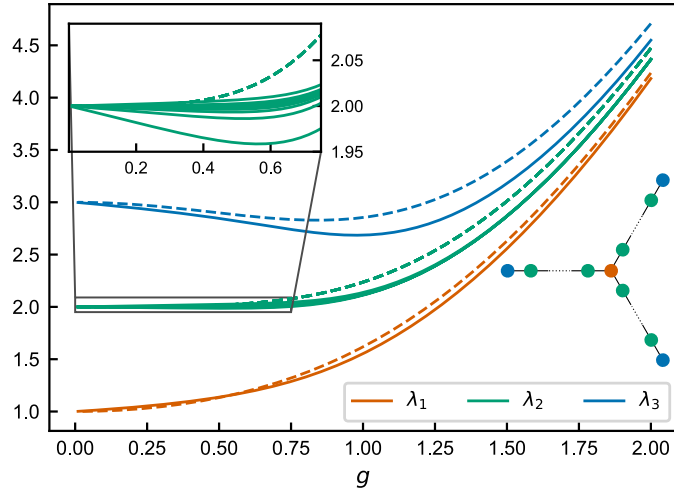


FIG. 2. Saddle point values of the Lagrange multipliers λ_i corresponding to sites with i neighbors of the Quantum Rotor model at $T = 0$ in the large n limit on a Y graph (solid lines) as a function of the coupling g (defined as in [48]). The solution depends on the position inside the leg of the junction. In contrast the classical model only depends on the number of neighbors (dashed lines). Temperature T in the classical model can be identified with g^2 of the quantum model by direct comparison.

The fact that the constraint equations can be solved for any tree is one of the main results of the paper, extending the classical result [47] of the $O(n)$ model on an open chain. Tree graphs explicitly highlight how both the Laplacian and the Adjacency matrix naturally emerge from the structure of M_{ij} :

$$M_{ij} \sim \begin{cases} KL_{ij}, & \text{for } K \rightarrow \infty, \\ KA_{ij} + \frac{1}{2}\delta_{ij}, & \text{for } K \rightarrow 0. \end{cases} \quad (12)$$

The local nature of the Lagrange multipliers is special to trees and does not generalize to most other graphs. Promoting the $O(n)$ model to the Quantum Rotor model [48] and taking the large n limit, this feature is lost as well (see Appendix D for more details). We illustrate this in Fig. 2, where the behavior of the Lagrange multipliers of both models on a Y graph is compared. In the classical model the Lagrange parameters λ_i only differ in sites with distinct z_i . In the quantum case, however, the λ_i of sites with the same coordination number (the sites within the chains of the Y structure) are different. Nevertheless, at high temperature they both tend to converge and reproduce the value λ_i of the classical model and their sole dependence on z_i . Moreover, also for $T \rightarrow 0$ they approach the same value, to reproduce a behavior determined solely by the Laplacian matrix.

VI. DECORATED LATTICE

A simple way to partially break translational invariance is to consider hypercubic lattices with decorations. This has been studied in [36] focusing on the critical temperature T_c as the number of decorations between sites grows. For simplicity, we consider here just one decoration in $d = 3$ dimensions such that every site has either two or 6 neighbors, but the calculations can easily be generalized. There are two types of sites: decorating sites, with Lagrange multiplier λ_d , and bulk sites of the underlying cubic lattice with Lagrange multiplier λ_l . Every decorating spin S_d is connected to two spins of the underlying cubic lattice such that it can be integrated out. In the thermodynamic limit the two

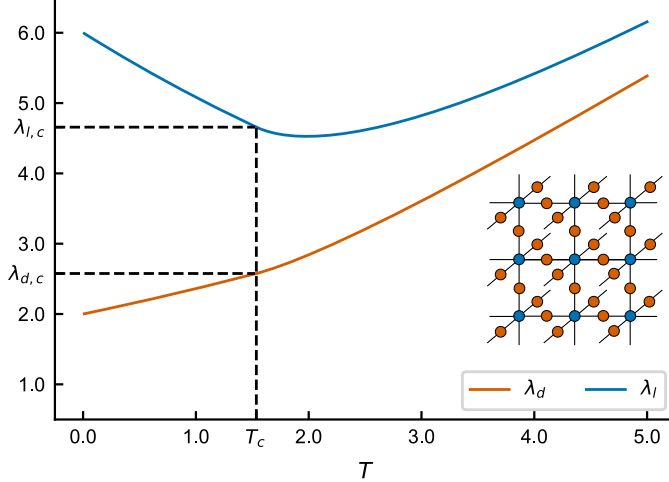


FIG. 3. Saddle point values of the Lagrange multipliers on a decorated lattice in three dimensions. Lagrange multipliers corresponding to decorating sites are denoted by λ_d , while the ones associated to the sites of the underlying lattice by λ_l . Above T_c , Eqs. (13) and (14) must be used, while below T_c one has to minimize (16).

constraint equations read:

$$K = \frac{\lambda_d}{2} \int \frac{d^3 k}{(2\pi)^3} \frac{1}{\frac{\lambda_d \lambda_l}{2} - 3 - \sum_{i=1}^3 \cos k_i}, \quad (13)$$

$$3K = \frac{2}{\lambda_d} + \frac{\lambda_l}{2} \int \frac{d^3 k}{(2\pi)^3} \frac{1}{\frac{\lambda_d \lambda_l}{2} - 3 - \sum_{i=1}^3 \cos k_i}, \quad (14)$$

where the Lagrange multipliers have been rescaled by K compared to the definition in the previous section. A detailed derivation is provided in Appendix E. It is easy to see that at $K = K_c$ one needs to have $\lambda_l^{(c)} \lambda_d^{(c)} = 12$. One can also convince themselves that the solutions to (13) and (14) are different from the Laplacian ones:

$$\lambda_l^{(c)} \neq 6, \quad \lambda_d^{(c)} \neq 2. \quad (15)$$

In the standard spherical model, the Lagrange multiplier sticks to its critical value below T_c . However, if one has more than one parameter, this is no longer the case since only the condition for criticality, in this case $\lambda_l \lambda_d = 12$, must be satisfied. The free energy must be minimized, under this constraint. The formerly non-analytic part is absorbed in the constant A and the free energy can be expressed as:

$$-\beta f = 2 \ln \lambda_d - 3 \lambda_d K - \frac{12K}{\lambda_d} + A. \quad (16)$$

Minimizing the free energy with respect to λ_d gives the correct behavior in the $K \rightarrow \infty$ limit. The resulting dependence of λ_l and λ_d on K is shown in Fig. 3. The two Lagrange multipliers converge for high temperatures and take on a non-trivial value at T_c . They approach their Laplacian values $\lambda_l = 6$ and $\lambda_d = 2$, while maintaining $\lambda_l \lambda_d = 12$, in the limit of zero temperature.

VII. STRIP

An example where the Lagrange multipliers yield a non-trivial Laplacian matrix in the whole low temperature phase was studied in [37]. There, a three dimensional strip of length L and periodic boundary conditions in the other two directions such that all sites have six neighbors except the boundary sites which have five, was considered. It was shown that, as long as

$$4\pi(K - K_c) \gg \frac{\log L}{L}, \quad (17)$$

where K_c is the bulk critical temperature, is fulfilled, one obtains approximately the Laplacian matrix in the low temperature regime. Therefore, the low temperature expansion is correct even close to T_c as long as L is sufficiently large. This arises from the fact that the fraction of boundary sites approaches zero in the $L \rightarrow \infty$ limit. In the classes we have explored we did not find other graphs governed by the Laplacian matrix throughout the low temperature regime, which further strengthens the claim that in general the Laplacian is approached in a non-trivial way in the zero temperature limit.

VIII. COMPLETE BIPARTITE GRAPH

For graphs with finite coordination numbers, the singular part of the model requires the Laplacian matrix [27]. We show that if one relaxes this condition one can obtain surprising behavior, namely that the critical behavior is determined by the Adjacency matrix. To illustrate this, we chose a bipartite graph where subset $A(B)$ has $N(2N)$ sites. All sites of subset A are connected to all sites of B . In this way, the coordination number of each site grows as $2N(N)$. The Hamiltonian is given by:

$$-\beta H = \frac{K}{N} \left(\sum_{j=1}^{2N} \sum_{i=1}^N S_{i,A} S_{j,B} \right) - \lambda_A \sum_{i=1}^N S_{i,A}^2 - \lambda_B \sum_{i=1}^{2N} S_{i,B}^2, \quad (18)$$

where the coupling has been rescaled by N to obtain extensive quantities. The spherical constraints can be solved analytically because of the simple structure of the graph and one arrives at (see Appendix F):

$$\lambda_A = \lambda_B = \frac{1}{2}, \quad \text{for } K \leq K_c = \frac{1}{2}, \quad (19)$$

implying that the Adjacency matrix determines the behavior in the whole high-temperature phase. Below T_c on the other hand, the solutions approach the correct ratio $\lambda_A/\lambda_B = 2$ for $K \rightarrow \infty$:

$$\begin{aligned} \lambda_A &= \frac{1}{4} \left(-1 + \sqrt{1 + 64K^2} \right), & \text{for } K \geq K_c, \\ \lambda_B &= \frac{1}{8} \left(1 + \sqrt{1 + 64K^2} \right), & \text{for } K \geq K_c. \end{aligned} \quad (20)$$

Therefore, one still obtains the general structure of Laplacian and Adjacency matrix for this graph with diverging coordination numbers.

IX. CONCLUSIONS

We have shown that the behavior of the $O(n)$ model in the large n limit on general graphs can be understood as a interplay between the Adjacency and Laplacian matrices. At high temperatures, the spectrum of the Adjacency matrix determines the free energy, while at low temperatures the Laplacian spectrum governs it. This behavior is enforced by a set of saddle point equations that simplify in the two temperature limits, where the Lagrange multipliers either approach the local coordination numbers z_i or become equal across sites. This contrasts with the usual definition of the spherical model on graphs, which assumes a single Lagrange multiplier multiplying the matrix $Z_{ij} = z_i \delta_{ij}$.

We illustrated this result on several representative graphs, both with and without phase transitions. For trees, the Lagrange multipliers were determined analytically, while for decorated lattices we showed how they remarkably approach their Laplacian values in the low temperature phase. For a graph with diverging coordination number, we demonstrated that the parameters remain fixed at their Adjacency matrix values even at the critical temperature T_c .

The large n analysis developed here provides a natural foundation for a $1/n$ expansion on graphs, enabling both the study of critical behavior and the calculation of non-universal quantities. Extending our results to the antiferromagnetic case, especially on graphs that allow frustration, will be particularly interesting, since there the low temperature limit is not simply governed by the Laplacian. Finally, the same framework can be extended to the quantum regime. In the large n limit of the $O(n)$ quantum rotor model on graphs, we expect the resulting saddle point equations and Lagrange multipliers again to reveal regimes dominated by the Laplacian or Adjacency spectra.

ACKNOWLEDGMENTS

The authors acknowledge funding from the European Union’s Horizon Europe Research and Innovation Programme under the Marie Skłodowska-Curie Doctoral Network MAWI (Matter-Wave Interferometers) under the grant agreement No. 101073088.

- [1] J. Cardy, *Scaling and Renormalization in Statistical Physics*, Cambridge Lecture Notes in Physics (Cambridge University Press, Cambridge, UK, 1996).
- [2] A. Zee, *Quantum Field Theory in a Nutshell*, 2nd ed. (Princeton University Press, Princeton, NJ, 2010).
- [3] S. H. Simon, *The Oxford Solid State Basics* (Oxford University Press, Oxford, UK, 2013).
- [4] P. M. Chaikin and T. C. Lubensky, *Principles of Condensed Matter Physics* (Cambridge University Press, Cambridge, UK, 1995).
- [5] D. ben Avraham and S. Havlin, *Diffusion and Reactions in Fractals and Disordered Systems* (Cambridge University Press, Cambridge, UK, 2000).
- [6] M. Mézard and A. Montanari, *Information, Physics, and Computation* (Oxford University Press, 2009).
- [7] M. Barthelemy, *Spatial Networks: A Complete Introduction: From Graph Theory and Statistical Physics to Real-World Applications* (Springer International Publishing, Cham, Switzerland, 2022).
- [8] R. Albert and A.-L. Barabási, Statistical mechanics of complex networks, *Reviews of Modern Physics* **74**, 47 (2002).
- [9] R. Burioni, D. Cassi, and A. Vezzani, Random walks and physical models on infinite graphs: an introduction, in *Random Walks and Geometry*, edited by V. A. Kaimanovich, K. Schmidt, and W. Woess (de Gruyter, Berlin, 2001) pp. 35–71.

- [10] Y. Gefen, B. B. Mandelbrot, and A. Aharony, Critical phenomena on fractal lattices, *Phys. Rev. Lett.* **45**, 855 (1980).
- [11] R. Rammal and G. Toulouse, Random walks on fractal structures and percolation clusters, *J. Physique Lett.* **44**, 13 (1983).
- [12] P. Monceau, Critical behavior of the ising model on random fractals, *Physical Review E* **84**, 051132 (2011).
- [13] C. Külske, The ising model: highlights and perspectives, *Mathematical Physics, Analysis and Geometry* **28**, 20 (2025).
- [14] G. Gauthier, I. Lenton, N. M. Parry, M. Baker, M. J. Davis, H. Rubinsztein-Dunlop, and T. W. Neely, Direct imaging of a digital micro-mirror device for configurable microscopic optical potentials, *Optica* **3**, 1136 (2016).
- [15] A. Smith, T. Easton, V. Guerrera, and G. Barontini, Generation of optical potentials for ultracold atoms using a superluminescent diode, *Physical Review Research* **3**, 033241 (2021).
- [16] A. L. Gaunt and Z. Hadzibabic, Robust digital holography for ultracold atom trapping, *Scientific Reports* **2**, 721 (2012).
- [17] T. Harte, G. D. Bruce, J. Keeling, and D. Cassettari, A conjugate gradient minimisation approach to generating holographic traps for ultracold atoms, *Optics Express* **22**, 26548 (2014).
- [18] M. A. Norcia, A. W. Young, and A. M. Kaufman, Microscopic control and detection of ultracold strontium in optical-tweezer arrays, *Physical Review X* **8**, 041054 (2018).
- [19] F. S. Cataliotti, S. Burger, C. Fort, P. Maddaloni, F. Minardi, A. Trombettoni, A. Smerzi, and M. Inguscio, Josephson junction arrays with bose-einstein condensates, *Science* **293**, 843 (2001), <https://www.science.org/doi/pdf/10.1126/science.1062612>.
- [20] O. Morsch and M. Oberthaler, Dynamics of bose-einstein condensates in optical lattices, *Rev. Mod. Phys.* **78**, 179 (2006).
- [21] F. Buccheri, G. Bruce, A. Trombettoni, D. Cassettari, H. Babujian, V. Korepin, and P. Sodano, Holographic optical traps for atom-based topological Kondo devices, *New Journal of Physics* **18**, 075012 (2016).
- [22] P. Sodano, A. Trombettoni, P. Silvestrini, R. Russo, and B. Ruggiero, Inhomogeneous superconductivity in comb-shaped Josephson junction networks, *New Journal of Physics* **8**, 327 (2006).
- [23] P. Silvestrini, R. Russo, C. V. B. Ruggiero, C. Granata, S. Rombetto, M. Russo, M. Cirillo, A. Trombettoni, and P. Sodano, Topology-induced critical current enhancement in Josephson networks, *Physics Letters A* **370**, 499 (2007).
- [24] M. Lucci, V. Campanari, D. Cassi, V. Merlo, F. Romeo, G. Salina, and M. Cirillo, Quantum coherence in loopless superconductive networks, *Entropy* **24**, 10.3390/e24111690 (2022).
- [25] A. Lucas, Ising formulations of many NP problems, *Frontiers in Physics* **2**, 5 (2014).
- [26] M. X. Goemans and D. P. Williamson, Improved approximation algorithms for maximum cut and satisfiability problems using semidefinite programming, *J. ACM* **42**, 1115–1145 (1995).
- [27] R. Burioni, D. Cassi, and C. Destri, $n \rightarrow \infty$ Limit of $O(n)$ Ferromagnetic Models on Graphs, *Phys. Rev. Lett.* **85**, 1496 (2000).
- [28] T. Haug, R. Dumke, L.-C. Kwek, and L. Amico, Andreev-reflection and Aharonov–Bohm dynamics in atomtronic circuits, *Quantum Science and Technology* **4**, 045001 (2019).
- [29] A. Tokuno, M. Oshikawa, and E. Demler, Dynamics of One-Dimensional Bose Liquids: Andreev-Like Reflection at Y Junctions and the Absence of the Aharonov-Bohm Effect, *Phys. Rev. Lett.* **100**, 140402 (2008).
- [30] N. Crampé and A. Trombettoni, Quantum spins on star graphs and the Kondo model, *Nuclear Physics B* **871**, 526 (2013).
- [31] D. Giuliano, P. Sodano, A. Tagliacozzo, and A. Trombettoni, From four- to two-channel Kondo effect in junctions of XY spin chains, *Nuclear Physics B* **909**, 135 (2016).
- [32] M. Moshe and J. Zinn-Justin, Quantum field theory in the large N limit: a review, *Physics Reports* **385**, 69 (2003).
- [33] T. H. Berlin and M. Kac, The Spherical Model of a Ferromagnet, *Phys. Rev.* **86**, 821 (1952).
- [34] H. W. Lewis and G. H. Wannier, Spherical Model of a Ferromagnet, *Phys. Rev.* **88**, 682 (1952).
- [35] H. E. Stanley, Spherical Model as the Limit of Infinite Spin Dimensionality, *Phys. Rev.* **176**, 718 (1968).
- [36] B. A. Khoruzhenko, L. A. Pastur, and M. V. Shcherbina, Large-n limit of the Heisenberg model: The decorated lattice and the disordered chain, *Journal of Statistical Physics* **57**, 41–52 (1989).

- [37] D. Dantchev, J. Bergknoff, and J. Rudnick, Casimir force in the $O(n \rightarrow \infty)$ model with free boundary conditions, *Phys. Rev. E* **89**, 042116 (2014).
- [38] H. J. F. Knops, Infinite spin dimensionality limit for nontranslationally invariant interactions, *Journal of Mathematical Physics* **14**, 1918 (1973).
- [39] D. Cassi and L. Fabbian, The spherical model on graphs, *Journal of Physics A: Mathematical and General* **32**, L93 (1999).
- [40] F. Harary, *Graph Theory* (Addison-Wesley Publishing Company, Boston, 1969).
- [41] J. A. Bondy and U. S. R. Murty, *Graph Theory with Applications* (Macmillan Press Ltd, London and New York, 1976).
- [42] R. Merris, Laplacian matrices of graphs: a survey, *Linear Algebra and its Applications* **197-198**, 143 (1994).
- [43] R. Burioni, D. Cassi, M. Rasetti, P. Sodano, and A. Vezzani, Bose-einstein condensation on inhomogeneous complex networks, *Journal of Physics B: Atomic, Molecular and Optical Physics* **34**, 4697 (2001).
- [44] I. Brunelli, G. Giusiano, F. P. Mancini, P. Sodano, and A. Trombettoni, Topology-induced spatial bose-einstein condensation for bosons on star-shaped optical networks, *Journal of Physics B: Atomic, Molecular and Optical Physics* **37**, S275 (2004).
- [45] R. Burioni and D. Cassi, Random walks on graphs: ideas, techniques and results, *Journal of Physics A: Mathematical and General* **38**, R45 (2005).
- [46] A. P. Millán, G. Gori, F. Battiston, T. Enss, and N. Defenu, Complex networks with tuneable spectral dimension as a universality playground, *Phys. Rev. Res.* **3**, 023015 (2021).
- [47] H. E. Stanley, Exact Solution for a Linear Chain of Isotropically Interacting Classical Spins of Arbitrary Dimensionality, *Phys. Rev.* **179**, 570 (1969).
- [48] T. Vojta, Quantum version of a spherical model: Crossover from quantum to classical critical behavior, *Phys. Rev. B* **53**, 710 (1996).

Appendix A: Large n Limit on General Graphs

The $O(N)$ model defined on a graph with Adjacency matrix A has the Hamiltonian:

$$-\beta H = K \sum_{i,j=1}^N A_{ij} \mathbf{S}_i \cdot \mathbf{S}_j = K \sum_{i,j=1}^N \sum_{a=1}^n S_{i,a} S_{j,a}. \quad (\text{A1})$$

We normalize the spins according to:

$$\sum_{a=1}^n S_{i,a}^2 = n. \quad (\text{A2})$$

The partition function reads:

$$Z = \int \prod_{i=1}^N \prod_{a=1}^n dS_{i,a} \exp \left(K \sum_{i,j=1}^N \sum_{a=1}^n S_{i,a} S_{j,a} \right) \prod_{i=1}^N \delta \left(n - \sum_{a=1}^n S_{i,a}^2 \right), \quad (\text{A3})$$

$$= \int \prod_{i=1}^N \prod_{a=1}^n dS_{i,a} \frac{1}{(2\pi i)^N} \int_{-i\infty}^{i\infty} \prod_{i=1}^N d\lambda_i \exp \left(K \sum_{i,j=1}^N \sum_{a=1}^n S_{i,a} S_{j,a} + \sum_{i=1}^N \lambda_i (1 - S_{i,a}^2) \right). \quad (\text{A4})$$

Since all components of the vectors \mathbf{S}_i are equivalent, one can drop the index and write

$$Z = \frac{1}{(2\pi i)^N} \int_{-i\infty}^{i\infty} \prod_{i=1}^N d\lambda_i \left\{ \int \prod_{i=1}^N dS_i \exp \left(K \sum_{i,j} S_i S_j + h \sum_i S_i + \sum_i \lambda_i (1 - S_i^2) \right) \right\}^n. \quad (\text{A5})$$

The integral over spins can readily be performed since it is Gaussian and in the large n limit one can use the saddle point approximation for the λ_i integrals. The only difference to the translational invariant case [35] is that λ_i cannot be replaced by a collective λ . The free energy is defined as

$$-\beta f = \lim_{n \rightarrow \infty} \frac{\log Z}{nN} \quad (\text{A6})$$

and the saddle point equations read:

$$\frac{\partial f}{\partial \lambda_i} = 0, \quad \text{for } i = 1, \dots, N. \quad (\text{A7})$$

Appendix B: Derivation of the Low- and High-Temperature Limits

Here we present a derivation of the limits (7) and (8). We start from the Hamiltonian (5) with an external field $h > 0$:

$$-\beta H \equiv \sum_{i,j=1}^N S_i (KA_{ij} - \delta_{ij} \lambda_i) S_j + h \sum_i S_i. \quad (\text{B1})$$

In the zero temperature limit the system occupies the ground state which can be found by solving:

$$0 = 2K \sum_{j \in A_i} S_j - 2\lambda_i S_i + h, \quad 0 = 1 - S_i^2, \quad (\text{B2})$$

where A_i is the set of sites connected S_i . The minimum energy solution is then given by:

$$S_i = 1, \quad \lambda_i = z_i K + \frac{h}{2}, \quad (\text{B3})$$

which for zero field is equal to Eq. (7) in the main text.

The Lagrange multipliers in the high temperature limit are most easily obtained by writing the partition function in terms of the determinant of M :

$$Z = \int \prod_{i=1}^N dS_i \exp \left(\sum_{i,j=1}^N S_i (KA_{ij} - \delta_{ij} \lambda_i) S_j \right) = \int \prod_{i=1}^N dS_i \exp \left(- \sum_{i,j=1}^N S_i M_{ij} S_j \right) = \sqrt{\frac{\pi^N}{\det M}}. \quad (\text{B4})$$

The determinant can be expanded up to first order in K :

$$\det M = \det(\text{diag}(\lambda_1, \dots, \lambda_N) - KA) \quad (\text{B5})$$

$$= \prod_{i=1}^N \lambda_i (1 + K \text{Tr}[A \cdot \text{diag}(1/\lambda_1, \dots, 1/\lambda_N)] + \mathcal{O}(K^2)) \quad (\text{B6})$$

$$= \prod_{i=1}^N \lambda_i + \mathcal{O}(K^2). \quad (\text{B7})$$

The saddle point equations in terms of the determinant are given by:

$$\det M = \frac{1}{2} \frac{\partial}{\partial \lambda_i} \det M, \quad (\text{B8})$$

such that the solution to first order simply reads:

$$\lambda_i = \frac{1}{2} + \mathcal{O}(K^2) \quad (\text{B9})$$

Appendix C: Large n Limit on Trees

To obtain the Lagrange parameters for a general tree we start with the partition function:

$$Z = \int \prod_{i=1}^N dS_i \exp \left(- \sum_{i,j=1}^N S_i (\delta_{ij} \lambda_i - KA_{ij}) S_j + \sum_{i=1}^N \lambda_i \right). \quad (\text{C1})$$

We now use the fact that in a tree there is always at least one leaf node S_k that is connected to only one other node $S_{k'}$ and separate these terms from the rest:

$$Z = \int \prod_{i=1}^N dS_i \exp \left(- \sum_{i,j \neq k}^N S_i (\delta_{ij} \lambda_i - KA_{ij}) S_j + \sum_{i \neq k}^N \lambda_i - \lambda_k S_k^2 + 2KS_k S_{k'} + \lambda_k \right). \quad (\text{C2})$$

Next, one performs the integral over S_k :

$$Z = \sqrt{\frac{\pi}{\lambda_k}} e^{\lambda_k} \int \prod_{i \neq k}^N dS_i \exp \left(- \sum_{i,j \neq k}^N S_i \left(\delta_{ij} \left(\lambda_i - \delta_{ik'} \frac{K^2}{\lambda_k} \right) - KA_{ij} \right) S_j + \sum_{i \neq k}^N \lambda_i \right), \quad (\text{C3})$$

and shifts the Lagrange multipliers:

$$\tilde{\lambda}_i = \lambda_i - \delta_{ik'} \frac{K^2}{\lambda_k}. \quad (\text{C4})$$

Thus, the partition function becomes:

$$Z = \sqrt{\frac{\pi}{\lambda_k}} e^{\lambda_k + \frac{K^2}{\lambda_k}} \int \prod_{i \neq k}^N dS_i \exp \left(- \sum_{i,j \neq k}^N S_i \left(\delta_{ij} \tilde{\lambda}_i - KA_{ij} \right) S_j + \sum_{i \neq k}^N \tilde{\lambda}_i \right). \quad (\text{C5})$$

This isolates λ_k , so that its saddle point equation reads:

$$\frac{1}{2\lambda_k} = -\frac{K^2}{\lambda_k^2} + 1, \quad (\text{C6})$$

whose solution is:

$$\lambda_k = \frac{1}{4} \left(1 + \sqrt{1 + 16K^2} \right). \quad (\text{C7})$$

All leaf nodes of the original tree share this Lagrange multiplier. The remaining graph is still a tree and therefore must contain at least one leaf node S_p . Since S_p was not a leaf in the first step, it must have been connected to $z_p - 1$ leaf nodes, where z_p is the sites coordination number. Its original Lagrange multiplier is, therefore, given by:

$$\lambda_p = \frac{1}{4} \left(1 + \sqrt{1 + 16K^2} \right) + (z_p - 1) \frac{K^2}{\frac{1}{4} (1 + \sqrt{1 + 16K^2})} \quad (\text{C8})$$

$$= \frac{1}{2} + \frac{z_p}{4} \left(-1 + \sqrt{1 + 16K^2} \right) \quad (\text{C9})$$

in agreement with Eq. (11) in the main text. The remaining graph can be integrated in the same way. The key point is that, at each step, only the sites directly connected to the leaf nodes are affected.

The Gaussian integrals also reveal that the determinant of M has the simple form:

$$\det M = \left[\frac{1}{4} \left(1 + \sqrt{1 + 16K^2} \right) \right]^{\frac{N-1}{2}}, \quad (\text{C10})$$

which together with

$$\sum_{i=1}^N \lambda_i = \sum_{i=1}^N \left[\frac{1}{2} + \frac{z_i}{4} \left(-1 + \sqrt{1 + 16K^2} \right) \right] = \frac{N-1}{4} \left(-1 + \sqrt{1 + 16K^2} \right) + \text{const}, \quad (\text{C11})$$

allows one to obtain the free energy

$$-\beta f = \frac{N-1}{N} \left[\frac{1}{4} \sqrt{1 + 16K^2} - \frac{1}{2} \log \left(1 + \sqrt{1 + 16K^2} \right) + \text{const} \right]. \quad (\text{C12})$$

Appendix D: Large n Limit for the $O(n)$ Quantum Rotor Model on a Y graph

In the main text, we compare the classical $O(n)$ model and the $O(n)$ quantum rotor model in the large n limit on a Y graph. We write the Hamiltonian of the quantum rotor model in the large n limit as [48]:

$$H = - \sum_{\langle ij \rangle} \hat{S}_i \hat{S}_j + \frac{g}{2} \sum_i \hat{P}_i^2 + \sum_i \lambda_i (\hat{S}_i^2 - 1). \quad (\text{D1})$$

The operators follow canonical commutation relations

$$[\hat{S}_i, \hat{S}_j] = [\hat{P}_i, \hat{P}_j] = 0, \quad [\hat{S}_i, \hat{P}_j] = i\delta_{ij}. \quad (\text{D2})$$

The free energy associated with Eq. (D1) can be straightforwardly calculated:

$$F = -T \sum_k \ln \sinh \left(\sqrt{\frac{g\Lambda_k}{2}} \frac{1}{T} \right) + \frac{1}{2} \sum_i (\lambda_i - g), \quad (\text{D3})$$

where Λ_k are the eigenvalues of M :

$$M_{ij} = -A_{ij} + \delta_{ij} \lambda_i. \quad (\text{D4})$$

We restrict ourselves to the zero temperature regime such that the free energy reads:

$$f = -\sqrt{\frac{g}{2}} \sum_k \sqrt{\Lambda_k} + \frac{1}{2} \sum_i (\lambda_i - g). \quad (\text{D5})$$

The saddle point equations are obtained through differentiation with respect to λ_i :

$$1 = \sqrt{\frac{g}{2}} \sum_k \frac{\Psi_{k,i}^2}{\sqrt{\Lambda_k}}, \quad (\text{D6})$$

where $\Psi_{k,i}$ is the i -th component of the k -th eigenvector of M . The main difference to the classical case is that in general one cannot write the saddle point equations in terms of the determinant, but instead is forced to consider the whole spectrum.

Appendix E: Decorated lattice

In the main text, we consider a three dimensional cubic lattice with a single decoration between each site. This is a special case of the decorated lattices considered in [36]. The Hamiltonian reads:

$$-\beta H = K \sum_{\langle S_l, S_d \rangle} S_l S_d + \sum_{i=1}^N \lambda_l (1 - S_{l,i}^2) + \sum_{j=1}^{3N} \lambda_d (1 - S_{d,j}^2). \quad (\text{E1})$$

The first sum runs over all bonds and can be written in this way because there are only connections between decorations S_d and cubic lattice sites S_l . We consider the problem of a single decoration because it simplifies the analysis while retaining the essential features we are interested in. Integrating each decorating spin yields an effective cubic lattice with modified interactions and additional diagonal terms. The individual integrals take the form:

$$\int_{-\infty}^{\infty} dS_d \exp(K(S_{l,1} + S_{l,2})S_d - \lambda_d S_d^2) = \sqrt{\frac{\pi}{\lambda_d}} \exp \left[\frac{K^2}{4\lambda_d} (S_{l,1}^2 + 2S_{l,1}S_{l,2} + S_{l,2}^2) \right]. \quad (\text{E2})$$

After performing all integrals over decorating sites, the partition function becomes

$$Z = \left(\frac{\pi}{\lambda_d} \right)^{\frac{3N}{2}} e^{N\lambda + 3N\lambda_d} \int \prod_{i=1}^N dS_{l,i} \exp \left[\sum_{\langle i,j \rangle} \frac{K^2}{2\lambda_d} S_{l,i} S_{l,j} - \sum_{i=1}^N \left(\lambda_l - \frac{3K^2}{2\lambda_d} \right) S_{l,i}^2 \right], \quad (\text{E3})$$

where $\langle i, j \rangle$ now denotes to the usual nearest neighbor sum on a cubic lattice. The remaining integrals can easily be evaluated by comparison with the known result for the three dimensional cubic lattice. After rescaling λ_l and λ_d by K , the free energy in the thermodynamics limit reads

$$-\beta f = 2 \ln \lambda_d - 3\lambda_d K - \lambda K + \int \frac{d^d k}{(2\pi)^d} \ln \left(\frac{\lambda_d \lambda}{2} - 3 - \sum_{i=1}^3 \cos k_i \right) + \text{const.} \quad (\text{E4})$$

By taking derivatives with respect to λ_l and λ_d one obtains the saddle point equations (13) and (14). At the critical point $\lambda_d^{(c)} \lambda_l^{(c)} = 12$ and the equations read:

$$K_c = \frac{\lambda_d^{(c)}}{2} K_{c,0}, \quad 3K_c = \frac{2}{\lambda_d^{(c)}} + \frac{\lambda_l^{(c)}}{2} K_{c,0}, \quad \lambda_d^{(c)} \lambda_l^{(c)} = 12, \quad (\text{E5})$$

where $K_{c,0}$ is the critical coupling of the three dimensional model without decoration and is given by a finite Watson integral:

$$K_{c,0} = \int \frac{d^3 k}{(2\pi)^3} \frac{1}{3 + \sum_{i=1}^3 \cos k_i}. \quad (\text{E6})$$

Solving the above system for K_c , λ_l and λ_d gives:

$$K_c = \frac{\sqrt{K_{c,0}} \sqrt{1 + 3K_{c,0}}}{\sqrt{3}}, \quad \lambda_l^{(c)} = \frac{6\sqrt{3K_{c,0}}}{\sqrt{1 + 3K_{c,0}}}, \quad \lambda_d^{(c)} = \frac{2\sqrt{1 + 3K_{c,0}}}{\sqrt{3}\sqrt{K_{c,0}}}. \quad (\text{E7})$$

Below T_c , we impose the condition $\lambda_l \lambda_d = 12$ to express the free energy in terms of a single Lagrange multiplier. Up to a constant A , the free energy reads:

$$-\beta f = 2 \ln \lambda_d - 3\lambda_d K - \frac{12K}{\lambda_d} + A. \quad (\text{E8})$$

The saddle point equation below T_c is given by:

$$0 = \frac{2}{\lambda_d} - 3K + \frac{12K}{\lambda_d^2}, \quad (\text{E9})$$

with the solution:

$$\begin{aligned} \lambda_l &= \frac{-1 + \sqrt{1 + (6K)^2}}{K}, & \text{for } K > K_c, \\ \lambda_d &= \frac{1 + \sqrt{1 + (6K)^2}}{3K}, & \text{for } K > K_c. \end{aligned} \quad (\text{E10})$$

The above expressions approach the expected Laplacian values $\lambda_l = 6$ and $\lambda_d = 2$ for $K \rightarrow \infty$.

Appendix F: Complete bipartite graph

We divide the nodes into two subsets A and B such that there are N nodes in A and $2N$ nodes in B . Afterwards all sites belonging to different subsets are connected. The Hamiltonian is given by:

$$-\beta H = \frac{K}{N} \left(\sum_{j=1}^{2N} \sum_{i=1}^N S_{i,A} S_{j,B} \right) + \lambda_A \sum_{i=1}^N (1 - S_{i,A}^2) + \lambda_B \sum_{i=1}^{2N} (1 - S_{i,B}^2). \quad (\text{F1})$$

The couplings are rescaled by N to obtain extensive thermodynamic quantities. The matrix M has the following structure:

$$M = \begin{pmatrix} D_A & -\frac{K}{N} J_{N \times 2N} \\ -\frac{K}{N} J_{2N \times N} & D_B \end{pmatrix}, \quad (\text{F2})$$

$$D_A = \text{diag}(\lambda_A, \dots, \lambda_A), \quad (\text{F3})$$

$$D_B = \text{diag}(\lambda_B, \dots, \lambda_B), \quad (\text{F4})$$

where $J_{N \times M}$ is the $N \times M$ matrix with all elements equal to one. The determinant of M can be calculated by using first a identity for block matrices:

$$\det \begin{pmatrix} A & B \\ C & D \end{pmatrix} = \det(A) \det(D - CA^{-1}B), \quad (\text{F5})$$

and then the determinant identity for $n \times n$ matrices of the form:

$$\det \begin{pmatrix} a & b & \dots & b \\ b & a & \ddots & \vdots \\ \vdots & \ddots & \ddots & b \\ b & \dots & b & a \end{pmatrix} = (a + (n-1)b)(a-b)^{n-1} \quad (\text{F6})$$

In the end, the determinant reads:

$$\det M = \lambda_A^{N-1} \lambda_B^{2N-1} (\lambda_A \lambda_B - 2K^2). \quad (\text{F7})$$

This gives rise to the following saddle point equations:

$$N = \frac{N}{2\lambda_A} + \frac{\lambda_B}{\lambda_A \lambda_B - 2K^2}, \quad (\text{F8})$$

$$2N = \frac{N}{\lambda_B} + \frac{\lambda_A}{\lambda_A \lambda_B - 2K^2}. \quad (\text{F9})$$

In the $N \rightarrow \infty$ limit, these equations are solved by:

$$\lambda_A = \lambda_B = \frac{1}{2}, \quad \text{for } K < K_c = \frac{1}{2\sqrt{2}}. \quad (\text{F10})$$

As $K \rightarrow K_c$ one approaches a zero of the partition function. The correct way to proceed in the low temperature regime, is to fix $\lambda_A \lambda_B - 2K^2$ and minimize the regular part. This leads to the following equations:

$$0 = \lambda_A \lambda_B - 2K^2, \quad (\text{F11})$$

$$0 = \frac{1}{2\lambda_A} + 1 - \frac{4K^2}{\lambda_A}. \quad (\text{F12})$$

The solutions are:

$$\lambda_A = \frac{1}{4} (-1 + \sqrt{1 + 64K^2}) \quad (\text{F13})$$

$$\lambda_B = \frac{1}{8} (1 + \sqrt{1 + 64K^2}). \quad (\text{F14})$$

At the critical coupling K_c they are equal to 1/2 and for $K \rightarrow \infty$ their ratio approaches 2 as expected.